Korean J. Chem. Eng., **28**(3), 697-702 (2011)
DOI: 10.1007/s11814-010-0406-1

Onset of buoyancy-driven instability in a pure melt solidified from above

In Gook Hwang* and Min Chan Kim,†**

*Department of Chemical and Biochemical Engineering, University of Suwon, Hwaseong-si, Gyeonggi-do 445-743, Korea
**Department of Chemical Engineering, Jeju National University, Jeju 690-756, Korea
(*Received 22 June 2010 • accepted 20 August 2010*)

Abstract−When a pure liquid is solidified from above, convection may be induced in a thermally-unstable layer. The onset of buoyancy-driven convection during time-dependent solidification is investigated by using similarly transformed disturbance equations. The thermal disturbance distribution of the solid phase is approximated by WKB method, and the effects of various parameters on the stability condition of melt phase are analyzed theoretically. The present constant temperature cooling model gives more unstable results than the constant solidification velocity model of Smith [1].

Key words: Buoyancy Driven Convection, Solidification, Stefan Problem, Similar Transform

INTRODUCTION

The onset of convective instability in a horizontal fluid layer has been studied extensively. Recently, hydrodynamic stability associated with the solidification has attracted many researchers' interest [1-11], because solid-liquid phase-change heat transfer is of interest to geophysical and engineering problems. The convective motion driven by buoyancy forces in the presence of solid components plays an important role in industrial applications, such as manufacturing of composite materials and purification of metals, as well as in a wide range of systems in nature, such as seasonal freezing and melting of soil, lakes and rivers, artificial freezing of the ground as a construction technique for supporting poor soils, insulation of underground buildings, thermal energy storage in porous media and storage of frozen foods. Thus, a fundamental understanding of convective stability in such a range of applications is very important.

Convective motion near the phase changing interface affects the local temperature and concentration fields which control the geometric characteristics of the interface and solidification rate. Sparrow et al. [6] and Karcher and Müller [7] investigated the Rayleigh-Bénard stability problem with solidification and melting. They employed a static assumption where the temporal growth rate of velocity and temperature disturbances is assumed to be zero. Smith [1] examined the onset of convection driven by the thermal gradient under the solidifying interface during directional solidification of a pure liquid. Later, Hwang [3] extended Smith's [1] analysis in the liquid saturated in the porous medium. By employing the surface of solidification with constant speed, the coupled effects on stability arising from thermal convection and solidification of a single-component liquid was examined [1,3]. However, since the temperature at the solid phase should be decreased exponentially with the time, their system has little physical meaning.

In this study, time-dependent solidification of liquid cooled from above, the so-called Stefan problem, is considered. When the temperature profiles in solid and liquid phase and the solid layer thickness vary with time, the onset conditions of buoyancy-driven convection are analyzed. In the present study, time-dependent linearized disturbance equations are transformed similarly by using a similarity variable and are solved numerically.

†To whom correspondence should be addressed.
E-mail: mckim@cheju.ac.kr

THEORETICAL ANALYSIS

1. Governing Equations

The system considered here consists of a semi-infinite liquid layer cooled from above, as shown in Fig. 1. For time t≥0 the upper boundary of the liquid is supercooled at a constant temperature and then the solid layer grows from above. The coordinate system is fixed at the upper boundary, and the position of the solid/liquid interface is moving in the *Z*-direction. Then, the governing equations in the porous-saturated melt layer are given by

$$\nabla \cdot \mathbf{U} = 0, \tag{1}$$

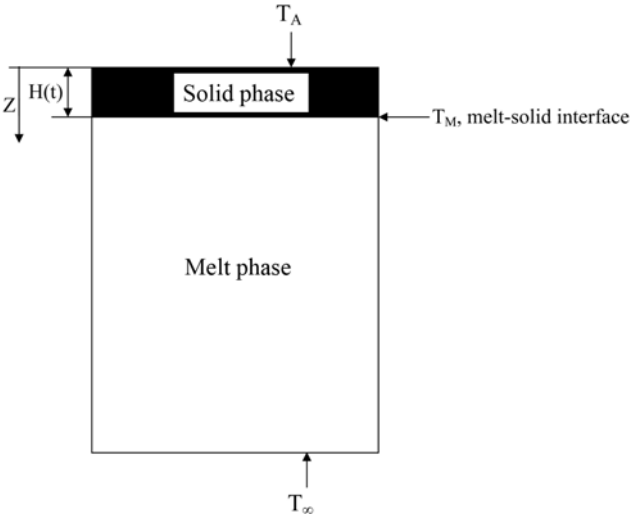

Fig. 1. Schematic diagram of system considered here.

$$\left\{\frac{\partial}{\partial t}+\mathbf{U}\cdot\nabla\right\}\mathbf{U}=-\nabla P+\mu\nabla^2\mathbf{U}+\rho\mathbf{g}, \tag{2}$$

$$\frac{\partial T_L}{\partial t}+\mathbf{U}\cdot\nabla T_L=\alpha_L\nabla^2 T_L, \tag{3}$$

$$\rho_L=\rho_r[1-\beta(T_L-T_r)], \tag{4}$$

where **U** denotes the velocity vector, μ the viscosity, P the pressure, ρ the density, β the thermal expansion coefficient, T the temperature, **g** the gravitational acceleration vector, t the time, and α the thermal diffusivity. The subscript L represents the liquid phase. And, for the solid layer, the temperature field can be described by

$$\frac{\partial T_S}{\partial t}=\alpha_S\nabla^2 T_S. \tag{4}$$

The subscripts L and S represent the liquid and solid phase, respectively. The boundary conditions are given as follows:

$$W=0,\ T_S=T_A \quad \text{at } Z=0, \tag{5}$$

$$T_S=T_L=T_M,\ k_S\frac{dT_S}{dZ}-k_L\frac{dT_L}{dZ}=L\frac{dH}{dt} \quad \text{at } Z=H(t), \tag{6(a) \& (b)}$$

$$T_L=T_\infty \quad \text{at } Z=\infty, \tag{7}$$

where L is the latent heat of melting and $H(t)(=\lambda\sqrt{4\alpha_L t})$ is the location of melt-solid interface. T_M denotes melting temperature at the solid-melt interface and T_∞ the temperature of melt far from the interface.

The basic thermal conduction equations are nondimensionalized as

$$\frac{\partial\theta_{0,S}}{\partial\tau}=\alpha_r\nabla^2\theta_{0,S}, \tag{8}$$

$$\frac{\partial\theta_{0,L}}{\partial\tau}+w_{0,L}\frac{\partial\theta_{0,L}}{\partial z}=\nabla^2\theta_{0,L}, \tag{9}$$

under the following boundary conditions:

$$\theta_{0,S}=-\frac{1+\theta_\infty}{\theta_\infty} \quad \text{at } z=0, \tag{10}$$

$$\theta_{0,S}=\theta_{0,L}=-1,\ k_r\frac{d\theta_{0,S}}{dz}-\frac{d\theta_{0,L}}{dz}=St\frac{dh}{d\tau} \quad \text{at } z=h(\tau), \tag{11(a),(b) \& (c))}$$

$$\theta_{0,L}=0 \text{ at } z=\infty, \tag{12}$$

where $w_{0,L}=-(\rho_r-1)(\lambda/\sqrt{\tau})$, $\theta_{0,S}=(T_S-T_\infty)/(T_\infty-T_M)$, $\theta_{0,L}=(T_L-T_\infty)/(T_\infty-T_M)$, $\theta_\infty=(T\infty-T_M)/T_M-T_A)$, $\tau=\alpha_L t/d^2$, $\alpha_r=\alpha_S/\alpha_L$, $k_r=k_S/k_L$, $z= Z/d$, $h=H/d$ the Stefan number $St=L/[c(T_\infty-T_M)]$ and d is an arbitrary length scale. The solution to the above equations and the boundary conditions are given in Carslaw and Jaeger's book [12]:

$$\theta_{0,S}=-\frac{1}{\theta_\infty}\left(1+\theta_\infty-\frac{\mathrm{erf}(\zeta/\sqrt{\alpha_r})}{\mathrm{erf}(\lambda/\sqrt{\alpha_r})}\right) \quad \text{for } \zeta<\lambda, \tag{13}$$

$$\theta_{0,L}=-\frac{\mathrm{erfc}\{\zeta\}}{\mathrm{erfc}\{\lambda\}} \quad \text{for } \zeta>\lambda, \tag{14}$$

where $\zeta=z/\sqrt{4\tau}$ and λ is the dimensionless position of solid-melt interface. The base temperature for the specific case is given in Fig. 2. The phase change rate λ can be determined by using Eqs. (11.c) (13) and (14) as:

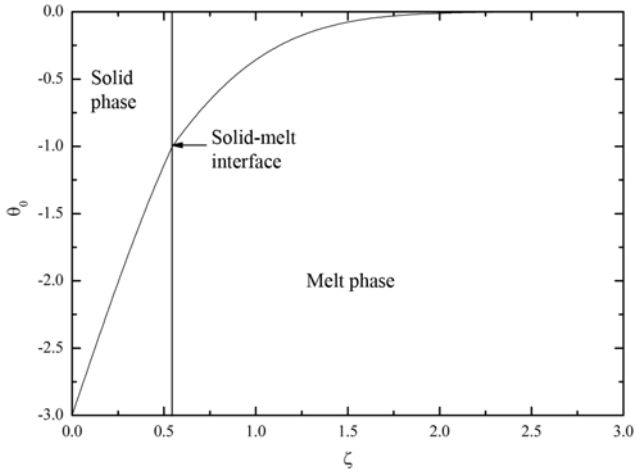

Fig. 2. Base temperature distribution for θ_∞=0.5, k_r=1 and α_r=1.

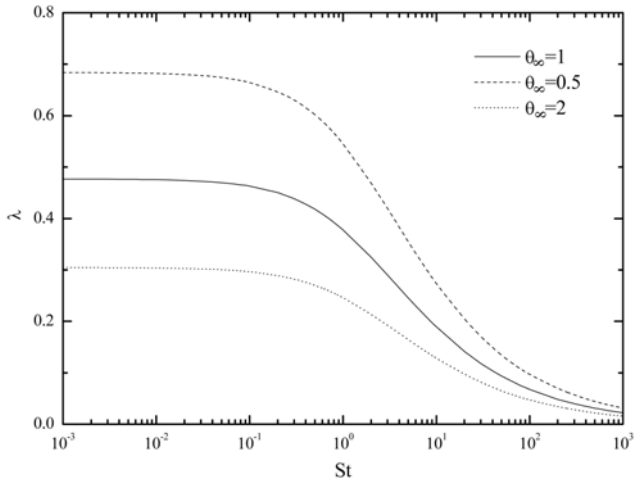

Fig. 3. Variation of phase change rate λ with the Stefan number St for k_r=1 and α_ρ=1.

$$\frac{k_r}{\theta_\infty\sqrt{\alpha_r}}\frac{\exp(-\lambda^2/\alpha_r)}{\mathrm{erf}(\lambda/\sqrt{\alpha_r})}-\frac{\exp(-\lambda^2)}{\mathrm{erfc}(\lambda)}=\lambda\sqrt{\pi}St, \tag{15}$$

and summarized as a function of St for some specific case in Fig. 3. Smith [1] and Hwang [3] assumed that the planar interface is moving with constant velocity V_0. According to their model, the temperature profiles are given as

$$\theta_{0,S}=-1-St\{1-\exp(-\eta/\alpha_r)\} \quad \text{for } \eta<0, \tag{16}$$

$$\theta_{0,L}=-\exp(-\eta) \quad \text{for } \eta>0, \tag{17}$$

where $\eta(=V_0(Z-V_0t)/\alpha_L)$ is the dimensionless vertical coordinate. Since the temperature at the top, $\theta_{0,S}=-1-St\{1-\exp(-V_0^2t/\alpha_S)\}$ decreases exponentially with the time, their system has little significance [12].

Under linear stability theory the physical variables are decomposed into unperturbed quantities and their perturbed ones at the onset of convection. In the melt layer the dimensionless disturbance equations are obtained as

$$\frac{\partial \theta_{1,L}}{\partial \tau} + R_T w_1 \frac{\partial \theta_{0,L}}{\partial z} = \nabla^2 \theta_{1,L}, \tag{13}$$

$$\left(\frac{1}{Pr}\frac{\partial}{\partial \tau} - \nabla^2\right)\nabla^2 w_1 = -\nabla_1^2 \theta_{1,L}, \tag{14}$$

where the subscript 1 denotes the perturbed quantities, the vertical velocity component, and R_T(=$g\beta\Delta T d^3/\alpha_L \nu$) the Rayleigh number. Note that θ_1 has the scale of $\alpha_L \nu/(g\beta d^3)$ and w_1 has the scale of α_L/d. In the solid layer the dimensionless disturbance equations are obtained as

$$\frac{\partial \theta_{1,S}}{\partial \tau} = \alpha_r \nabla^2 \theta_{1,S}. \tag{15}$$

The boundary conditions for these disturbances equations are given by

$$w_1 = \frac{\partial w_1}{\partial z} = \theta_{1,L} = 0 \quad \text{at } z=0. \tag{21}$$

$$w_1 = \frac{\partial w_1}{\partial z} = 0,\ \theta_{1,S} = \theta_{1,L},\ k_S D\theta_{1,S} = k_L D\theta_{1,L} \quad \text{at } z=h, \qquad (22(a),(b) \& (c))$$

$$\theta_{1,S} = 0 \quad \text{at } z=\infty, \tag{23}$$

In the present study the scaling of $W_1 \sim g\beta T_1 H^2/\nu$ in dimensional form is obtained from Eq. (2). This relation means that $w_1/\theta_1 \sim h^2 \sim \tau$. If disturbance amplitudes follow the property of the base temperature fields shown in the relations (10) and (11), it is probable that $\partial\theta_1/\partial\tau = -(2\zeta/\tau)(d\theta^*/d\zeta)$. Therefore, under the normal mode analysis the dimensionless amplitude functions of disturbances are assumed to have the relation of

$$[w_1, \theta_{1,L}, \theta_{1,S}] = [\delta^2 w^*(\zeta), \theta_L^*(\zeta), \theta_S^*(\zeta)]\exp[i(a_x x + a_y y)] \tag{17}$$

where a_x and a_y are the horizontal wavenumbers in the x and the y direction, respectively. The above equation means that the amplitude of dimensionless disturbances is assumed to be a function of the similarity variable ζ(=z/δ) where $\delta = \sqrt{4\tau}$. This kind of similarity transformation has been widely used in similar problems [4,13-15].

Substituting Eq. (24) into Eqs. (18)-(23) with $a^2 = a_x^2 + a_y^2$, $\partial/\partial\tau = -(2\zeta/\tau)D$ and $\partial^2/\partial z^2 = (1/4\tau)D^2$ gives the following self-similar stability equations:

$$\left(D^2 + \frac{2}{\alpha_r}\zeta D - a^{*2}\right)\theta_S^* = 0, \tag{18}$$

$$(D^2 + 2\zeta D - a^{*2})\theta_L^* = R_T^* w^* D\theta_{0,L}, \tag{19}$$

$$\left[(D^2 - a^{*2})^2 + \frac{2}{Pr}(\zeta D^3 - a^{*2}\zeta D + 2a^{*2})\right]w^* = -a^*\theta_L^*, \tag{20}$$

under the following boundary conditions:

$$w^* = Dw^* = \theta_L^* = 0 \quad \text{at } z=0, \tag{28}$$

$$w^* = Dw^* = 0,\ \theta_S^* = \theta_L^*,\ k_S D\theta_S^* = k_L D\theta_L^* \quad \text{at } z=l, \qquad (29(a),(b) \& (c))$$

$$w^* = Dw^* = \theta_L^* = 0 \quad \text{at } \zeta=\infty. \tag{30}$$

where $Ra^* = Ra\delta^3$, $a^* = a\delta$ and $D = d/d\zeta$. Ra^* and a^* are assumed to be eigenvalues having the meaning of the Darcy-Rayleigh number and the wave number based on the thermal penetration depth in liquid phase, $\Delta_T(\propto\sqrt{t})$. Through the similarity assumption of Eq. (24), $(2/\alpha_r)\zeta D\theta_S^*$ and $2\zeta D\theta_L^*$ occur in Eqs. (25) and (26), respectively. These terms have been neglected in quasi-static analysis, where the terms of $\partial(\cdot)/\partial\tau$ are assumed to be 0.

2. Solution Method

The stability equation for the solid layer can be solved independently of the melt layer by using the boundary conditions of Eq. (28). By using WKB approximation [16], the temperature disturbance in the solid layer can be approximated as:

$$\theta_S^* \sim \frac{\exp\left(-\frac{\zeta^2}{2\alpha_r}\right)}{\left(\frac{\zeta^2}{\alpha_r^2} + \frac{1}{\alpha_r} + a^{*2}\right)^{1/4}}\left[\exp\left\{\int_0^\zeta \left(\frac{\zeta^2}{\alpha_r^2} + \frac{1}{\alpha_r} + a^{*2}\right)^{1/2} d\zeta\right\} - \exp\left\{-\int_0^\zeta \left(\frac{\zeta^2}{\alpha_r^2} + \frac{1}{\alpha_r} + a^{*2}\right)^{1/2} d\zeta\right\}\right] \tag{31}$$

$$\theta_S^* \sim \frac{\exp\left(-\frac{\zeta^2}{2\alpha_r}\right)}{\left(\frac{\zeta^2}{\alpha_r^2} + \frac{1}{\alpha_r} + a^{*2}\right)^{1/4}}\left[\exp\left\{\frac{1}{\alpha_r}\frac{\zeta\sqrt{\zeta^2 + (\alpha_r + \alpha_r^2 a^2)}}{2}\right\}\left\{\frac{\zeta + \sqrt{\zeta^2 + (\alpha_r + \alpha_r^2 a^2)}}{\sqrt{(\alpha_r + \alpha_r^2 a^2)}}\right\}^{\frac{1+a^2\alpha_r}{2}} - \exp\left\{-\frac{1}{\alpha_r}\frac{\zeta\sqrt{\zeta^2 + (\alpha_r + \alpha_r^2 a^2)}}{2}\right\}\left\{\frac{\zeta + \sqrt{\zeta^2 + (\alpha_r + \alpha_r^2 a^2)}}{\sqrt{(\alpha_r + \alpha_r^2 a^2)}}\right\}^{\frac{-1-a^2\alpha_r}{2}}\right]$$

which satisfies the boundary condition of Eq. (28). And, then the boundary condition of Eqs. (29.b) and (29.c) can be reduced as:

$$D\theta_L^*(\lambda) = k_r\left[\left(\frac{\lambda^2}{\alpha_r^2} + \frac{1}{\alpha_r} + a^{*2}\right)^{1/2} f(\lambda, a^*, \alpha) - \frac{\lambda}{\alpha_r} - \frac{1}{2}\frac{\lambda}{\alpha_r^2}\left(\frac{\lambda^2}{\alpha_r^2} + \frac{1}{\alpha_r} + a^{*2}\right)^{-1}\right]\theta_L^*(\lambda) \tag{32}$$

where

$$f(\lambda, a^*, \alpha) = \frac{1 + \exp\left\{-2\int_0^\lambda \left(\frac{\zeta^2}{\alpha_r^2} + \frac{1}{\alpha_r} + a^{*2}\right)^{1/2} d\zeta\right\}}{1 - \exp\left\{-2\int_0^\lambda \left(\frac{\zeta^2}{\alpha_r^2} + \frac{1}{\alpha_r} + a^{*2}\right)^{1/2} d\zeta\right\}} = \frac{1 + \left(\frac{\sqrt{(1/\alpha_r + a^{*2})}}{\lambda/\alpha_r + \sqrt{(\lambda^2/\alpha_r^2 + 1/\alpha_r + a^{*2})}}\right)^{1+a^{*2}\alpha_r}\exp\sqrt{(\lambda^2/\alpha_r^2 + 1/\alpha_r + a^{*2})}}{1 - \left(\frac{\sqrt{(1/\alpha_r + a^{*2})}}{\lambda/\alpha_r + \sqrt{(\lambda^2/\alpha_r^2 + 1/\alpha_r + a^{*2})}}\right)^{1+a^{*2}\alpha_r}\exp\sqrt{(\lambda^2/\alpha_r^2 + 1/\alpha_r + a^{*2})}}$$

Through this procedure, the stability equations to be solved are Eqs. (26) and (27) under the boundary conditions of Eqs. (29.a) (30) and (32). For the limiting case of $k_r=0$ and $k_r=\infty$, the boundary conditions of Eq. (32) can be reduced $D\theta_L^*(\lambda)=0$ and $\theta_L^*(\lambda)=0$, respectively.

These stability equations are solved by employing the outward shooting scheme. For a given λ, k_r and α_r, in order to integrate these stability equations the proper values of Dw^* and θ^* at $\zeta=\lambda$ are assumed for a given a^*. Since the stability equations and their boundary conditions are all homogeneous, the value of $Dw^*(\lambda)$ can be assigned arbitrarily and the value of the parameter R_T^* is assumed. This procedure can be understood easily by taking into account the

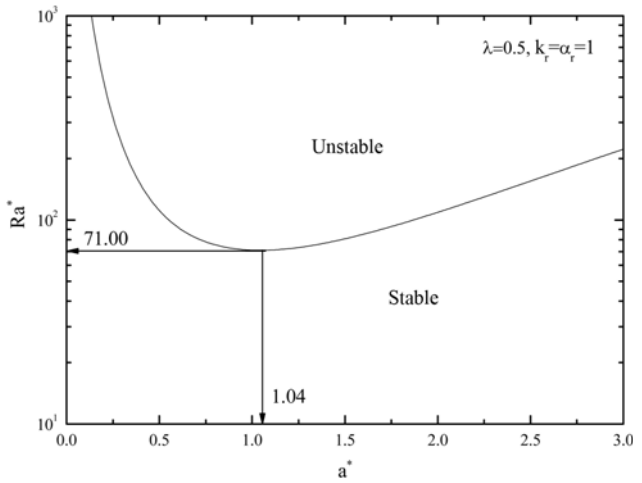

Fig. 4. Neutral stability curve for θ_∞=0.5, k_r=1 and α_r=1.

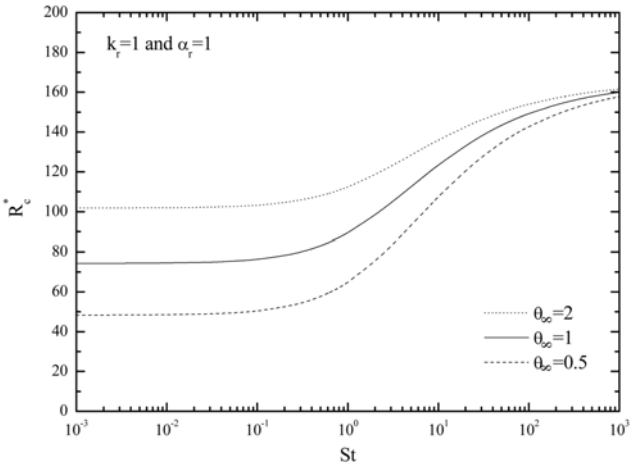

Fig. 5. Critical conditions for k_r=1 and α_r=1.

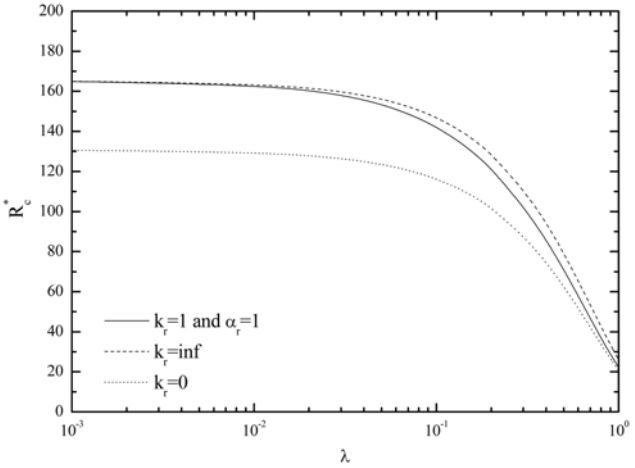

Fig. 6. The effect of λ on the critical conditions. Pr$\rightarrow\infty$.

characteristics of eigenvalue problems. After all the values at ζ=0 are provided, this eigenvalue problem can proceed numerically.

Integration is performed from a solid-melt interface $\zeta=\lambda$ to a fictitious outer boundary with the fourth order Runge-Kutta-Gill method. To improve the initial guesses the Newton-Raphson iteration is used. If the guessed values of R_T^* and $\theta_L^*(\lambda)$ are correct, the bounday conditions for w^* and θ^* will be satisfied at the fictitious outer boundary. Since disturbances decay superexponentially outside the thermal penetration depth as given in Eqs. (35) and (36), the incremental change of R_T^* also decays rapidly with increasing a fictitious outer boundary thickness. This behavior enables us to extrapolate the eigenvalue R_T^* to the infinite depth by using the Shanks transform. The marginal stability curve for the typical case is given in Fig. 4. The region above the curve denotes the unstable state, whereas that below the curve is stable state. In the figure the minimum value of R_T^* is the critical condition marking the onset of buoyancy-driven convection.

RESULTS AND DISCUSSION

The dimensionless parameters governing the present system are St, θ_∞, α_r and k_r. The effects of these parameters on convective instabilities during the solidification can be represented by λ through Eq. (15) and the boundary conditions of Eq. (32). For the case of k_r=1 and α_r=1, the effects of St and θ_∞ on the critical condition are summarized in Fig. 5. From Figs. 3 and 5, it can be known that the smaller the growth rate is, the more stable the system is. Since the temperature gradient near the solid-melt interface is given, $D\theta_{0,L}=-(2/\sqrt{\pi})(\exp(-\zeta^2/4))/(\mathrm{erfc}(\lambda))$, it can be expected that makes the system unstable through the large driven force.

For a given λ, the stability conditions of the limiting cases of $k_r=\infty$ and k_r=0 are given in Fig. 6. In these limiting cases the critical conditions are independent of α_r, since the boundary conditions of Eq. (32) can be reduced $D\theta_L^*(\lambda)$=0 for k_r=0 and $\theta_L^*(\lambda)$=0 for $k_r=\infty$. For the limiting case of small λ, the basic temperature profile becomes $\theta_{0,L}=-\mathrm{erfc}(\zeta)$ and the boundary conditions on the melt-solid interface become $\theta_L^*(\lambda)$=0 for the finite k_r. In this case of the small λ and finite k_r, the critical conditions approach asymptotically to Ra_c^*=165.38 and a_c^*=1.06. Kim et al. [14] analyzed the onset of buoyancy-driven convection in a fluid layer heated isothermally from below. Their stability equations which consider temporal growth of disturbances quantities are identical with the present ones by considering the scale of $\delta=\sqrt{4\tau}$ in the present analysis, and their stabil-

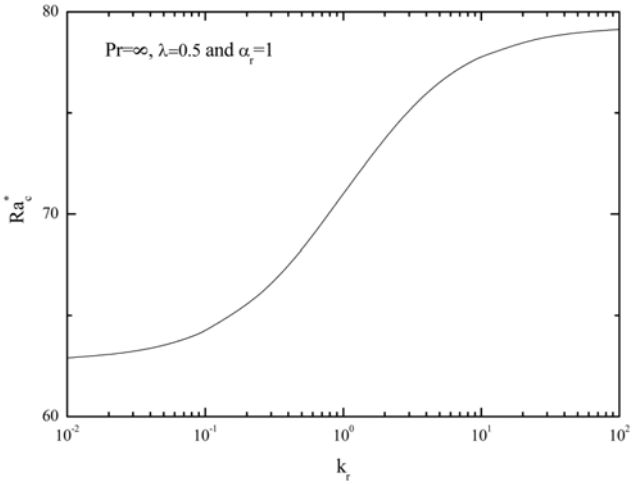

Fig. 7. The effect of k_r on the critical conditions for the case of λ=0.5.

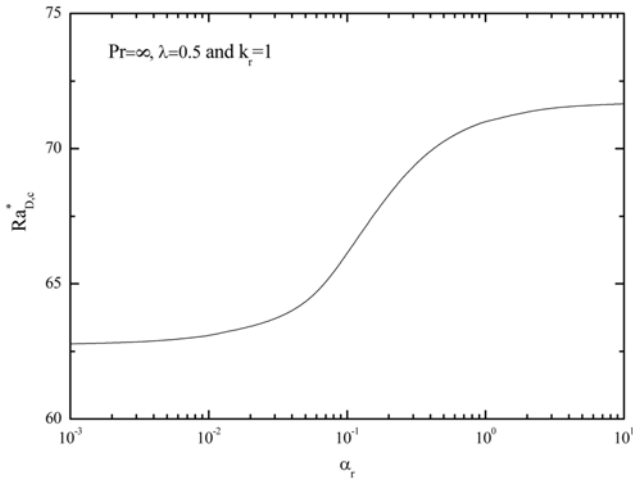

Fig. 8. The effect of α_r on the critical conditions for the case of λ= 0.5.

ity criteria of $Ra^*_{D,c}$=165.36 and a^*_c=1.06 in the present scale are quite similar to the present ones. This proves the validity of our solution method.

The effects of k_r on the critical conditions are summarized in Fig. 7 for various values of α_r with λ=0.5. The critical conditions approach the asymptotic values for $k_r=\infty$ and $k_r=0$. For large α_r case, the boundary condition of Eq. (32) reduces as $D\theta_L^*(\lambda)=k_r a^*(1+\exp(-2\lambda a^*))/(1-\exp(-2\lambda a^*))\theta_L^*(\lambda)$ and for small α_r case, it becomes $D\theta_L^*(\lambda)=0$. From this, it can be assumed that the effect of k_r on the critical condition is not significant for small α_r, as shown in Fig. 8. With increasing k_r and α_r, the critical Rayleigh number Ra_c^* increases and the system becomes more stable.

In the present system, the heat flux and from the sold-melt interface and the solidification velocity decrease like $t^{-1/2}$. Since this decrease of the heat removal accumulates the driving force for the onset of buoyancy-driven convection near the solid-melt interface, the present model gives more unstable results than the constant solidification velocity model of Smith [1] where the top temperature T_A should be decreased exponentially with the time to maintain the constant heat flux and from the sold-melt interface and the solidification velocity.

CONCLUSIONS

The onset of buoyancy-driven convection in a homogeneous melt solidified from above is analyzed by considering both the solid and melt phases. More realistic boundary conditions are applied and the effects of the various parameters are considered through the heat balance and the boundary conditions at the solid-melt interface. The stability characteristics are governed mainly by the heat removal through the solid phase. The large k_r and α_r enhance the heat removal and then stabilize the system. However, the large λ which can be obtained through the large latent heat accumulates the heat near the solid-melt interface and makes the system unstable.

NOMENCLATURE

a : dimensionless wavenumber, $\sqrt{a_x^2+a_y^2}$
a^* : modified dimensionless wave number, $a\delta$
a_H : dimensionless wave number based on the melt thickness, $a^*\lambda$
c : specific heat [J/(kg·K)]
d : arbitrary length scale [m]
g : gravitational acceleration vector [m/s^2]
H : thickness of the melt layer [m]
h : dimensionless thickness of the melt layer, H/d
K : permeability [m^2]
k : thermal conductivity [W/(m·K)]
k_r : thermal conductivity ratio, k_S/k_L
L : latent heat of melting [J/kg]
P : pressure [Pa]
Ra : Rayleigh number, $g\beta\Delta Td^3/\alpha_L\nu$
Ra^* : modified Rayleigh number, $Ra\delta^3$
Ra_H : Rayleigh number based on the melt thickness, $Ra^*\lambda$
St : Stefan number, $L/[c(T_A-T_M)]$
T : temperature [K]
t : time [s]
U : velocity vector [m/s]
w : dimensionless vertical velocity component
(x, y, z) : dimensionless Cartesian coordinates

Greek Letters

α : thermal diffusivity [m^2/s]
α_r : thermal diffusivity ratio, α_S/α_L
β : thermal expansion coefficient [K^{-1}]
δ : dimensionless depth, $\sqrt{4\tau}$
ε : porosity
θ : dimensionless temperature, $(T-T_A)/(T_A-T_M)$
λ : phase change rate
μ : viscosity [Pa·s]
ρ : density [kg/m^3]
τ : dimensionless time, $\alpha_L t/d^2$
ζ : similarity variable, z/δ

Subscripts

c : critical state
L : liquid phase
S : solid phase
0 : basic quantity
1 : perturbed quantity

REFERENCES

1. M. K. Smith, *J. Fluid Mech.*, **188**, 547 (1988).
2. G. Brandeis and B. D. Marsh, *Nature*, **339**, 613 (1989).
3. I. G. Hwang, *AIChE J.*, **47**, 1698 (2001).
4. I. G. Hwang and C. K. Choi, *J. Cryst. Growth*, **267**, 714 (2004).
5. X. Zhang and T. H. Nguyen, *Int. J. Numer. Methods Heat Fluid Flow*, **9**, 72 (1999).
6. E. M. Sparrow, L. Lee and N. Shamsundar, *J. Heat Transfer*, **98**, 88 (1976).
7. C. Karcher and U. Müller, *Fluid Dynamic Research*, **15**, 25 (1995).
8. J. A. Weaver and R. Viskanta, *Trans. ASME J. Heat Transfer*, **108**, 654 (1986).
9. C. Beckermann and R. Viskanta, *Int. J. Heat Mass Transfer*, **31**, 35

(1988).
10. D. V. Boger and J. W. Westwater, *Trans. ASME J. Heat Transfer*, **89**, 81 (1967).
11. X. Zhang and T. H. Nguyen R. Kahawita, *Int. J. Heat Mass Transfer*, **34**, 389 (1991).
12. H. S. Carslaw and J. C. Jaeger, Conduction of Heat in Solids, 2nd Ed., Oxford Univ. Press (1959).
13. M. C. Kim, D. W. Lee and C. K. Choi, *Korean J. Chem. Eng*., **25**, 1239 (2008).
14. M. C. Kim, H. K. Park and C. K. Choi, *Theoret. Comput. Fluid Dynamics*, **16**, 49 (2002).
15. M. C. Kim and S. G. Lee, *Korean J. Chem. Eng*., **26**, 21 (2009).
16. J. Mathews, R. L. Walker, Mathematical Methods of Physics, 2nd Ed., W.A. Benjamin Inc. (1970).